Frontiers in Bioscience Landmark

Front. Biosci. (Landmark Ed) **2026**; 31(5): 50041
https://doi.org/10.31083/FBL50041

Original Research

Arginine Promotes Antler Reserve Mesenchymal Cell Proliferation and Chondrogenesis via Altered Wnt/β-catenin and mTOR Signaling

Ruijia Deng[1,†], Yutong Zhang[1,†], Huanhuan Liu[1], Xing Duan[1], Hanlu Liu[2,3], Huazhe Si[1,3,*], Weixiao Nan[1,3,*]

[1]College of Animal Science and Technology, Jilin Agricultural University, 130118 Changchun, Jilin, China
[2]College of Agriculture, Chifeng University, 024000 Chifeng, Inner Mongolia Autonomous Region, China
[3]Joint International Research Laboratory of Modern Agricultural Technology, Ministry of Education, Jilin Agricultural University, 130118 Changchun, Jilin, China
*Correspondence: sihuazhe1989@163.com (Huazhe Si); nanweixiao@jlau.edu.cn (Weixiao Nan)
†These authors contributed equally.

Academic Editor: Francesca Diomede
Submitted: 15 January 2026 Revised: 16 April 2026 Accepted: 30 April 2026 Published: 26 May 2026

Abstract

Background: Arginine (Arg) is a functional amino acid implicated in tissue growth, but its effects on deer antler reserve mesenchymal cells (RMCs) remain unclear. **Methods**: We evaluated Arg-induced changes in the proliferation and chondrogenic differentiation of RMCs *in vivo* and *in vitro* and characterized the associated transcriptomic signatures. **Results**: Dietary supplementation with Arg increased the proportion of Ki67-positive cells in the mesenchymal cell–rich region of growing antlers. *In vitro*, Arg enhanced RMC viability and 5-Ethynyl-2′-deoxyuridine incorporation assay (EdU)incorporation in a dose-dependent manner, with 400 µM showing the strongest effect. RNA sequencing revealed broad transcriptional remodeling, with enrichment of extracellular matrix (ECM)/adhesion programs and growth-related pathways including PI3K-Akt, Wnt and mTOR signaling pathway. Arg also enhanced chondrogenic differentiation, as indicated by stronger Alcian blue staining and increased expression of SOX9 and COL2A1. During chondrogenic induction, Arg (800 µM) was associated with activation of mTOR signaling and attenuation of Wnt/β-catenin output. **Conclusions**: Collectively, these findings show that Arg promotes the expansion and chondrogenic differentiation of RMCs. Moreover, the Wnt/β-catenin and mTOR pathways are candidate signaling axes linked to Arg responses.

Keywords: mesenchymal stem cells; cell proliferation; β-catenin; mTOR; arginine

1. Introduction

Deer antlers represent a unique example of rapid and repeated organ regeneration in mammals, making them a key model for studying tissue growth, morphogenesis, and repair [1]. During antler development, the growth center produces cartilage at an unusually high rate [2]. This rapid chondrogenesis relies on a population of progenitor cells from the reserve mesenchyme that are capable of continual expansion and differentiation into various lineages [3]. Consequently, the proliferation and chondrogenic differentiation of antler reserve mesenchymal cells (RMCs) are crucial cellular processes that drive antler growth and tissue regeneration [4].

Chondrogenesis is governed by the coordinated regulation of lineage-determining transcriptional programs and assembly of the extracellular matrix (ECM) [5]. The transcription factor SOX9 is widely recognized as a master regulator of chondrocyte fate [6]. SOX9 drives the expression of key cartilage matrix genes such as *COL2A1* and promotes the deposition of cartilage-like ECM components, including glycosaminoglycans and proteoglycans [7]. In addition to transcriptional regulation, cartilage formation is strongly influenced by the extracellular microenvironment [8]. ECM receptor interactions and focal adhesion signaling, largely mediated by integrins and adhesion complexes, regulate cell adhesion and migration, mechanotransduction, and downstream gene expression programs [9]. These ECM-derived cues can also interact with canonical growth and differentiation pathways, including PI3K-Akt, Hippo signaling mediated by YAP and TAZ, mTOR, and Wnt signaling, thereby integrating mechanical cues, nutrient availability, and biosynthetic demand during cartilage development and regeneration [10,11]. However, it remains unclear how nutrient cues link to these regulatory networks and influence antler RMCs.

Arginine (Arg) is a conditionally essential amino acid that has multiple roles in regulating cell growth and metabolism [12]. Besides serving as a substrate for protein synthesis, Arg is an important precursor of nitric oxide and polyamines, as well as being involved in amino acid-sensing pathways that control anabolic signaling [13,14]. Importantly, the availability of Arg has been shown to affect nutrient-sensitive mTORC1 signaling through specific sensing mechanisms, thereby supporting cellular biosynthesis and proliferation [15]. An increasing number of studies have also suggested that Arg can influence stem and pro-

genitor cell behaviors and tissue repair processes by modulating growth signaling and metabolic states [15–17].

Based on this biological rationale, we previously conducted a feeding experiment using rumen-protected Arg [18]. This supplementation strategy was found to significantly increase circulating Arg levels and further improve antler yield, suggesting a potential causal relationship between Arg supply and antler growth. Although our *in vivo* phenotypic data support a promoting effect of Arg on antler production, the cellular targets, key transcriptional regulatory programs, and signaling networks that underlie this effect remain unclear. In particular, rapid antler growth depends on the sustained expansion and chondrogenic differentiation of RMCs, together with extensive ECM production and remodeling [19]. To elucidate the molecular mechanisms by which Arg promotes antler growth, one needs to systematically examine how it influences the proliferation and chondrogenic potential of RMCs at the cellular and molecular levels, as well as identify the associated transcriptional programs and signaling modules.

Therefore, the aims of this study were to investigate whether Arg promotes the proliferation of antler RMCs, how it reshapes their transcriptomic profiles, how it enhances chondrogenic differentiation, and whether it is associated with changes in pathway-related signaling signatures.

2. Materials and Methods

2.1 Animals, Experimental Design, and Diets

The experimental protocol was approved by the Animal Ethics Committee of Jilin Agricultural University (Approval ID: 20220614005). Sixteen healthy, four-year-old male sika deer (*Cervus nippon*, average body weight: 108 ± 4.5 kg), with the same antler casting date (approximately 15 May 2023). The animals were randomly allocated into two experimental groups (n = 8 per group). All animals were fed a total mixed ration (TMR) consisting of 45% roughage and 55% concentrate on a dry matter basis (for detailed composition, see **Supplementary Table 1**). The control group received the basal diet, while the treatment group was given the same basal diet supplemented with 3.0 g/day of rumen-protected arginine. Each deer was housed individually and fed twice daily at 07:00 and 16:00, with free access to clean water. The experiment was conducted over an 8-week period following hard antler removal, which included a one-week dietary adaptation phase and a seven-week formal treatment phase. Antler mesenchymal tissue was subsequently collected. Antler mesenchymal tissue was then collected, with a portion immediately fixed for Immunofluorescence and the remaining tissue was placed in PBS for the isolation of RMCs. Animal health and welfare were monitored throughout the experiment by trained personnel under veterinary supervision. Appetite/feed intake, water intake, demeanor, locomotor activity, body condition, wound condition, bleeding, signs of infection, and pain-related behaviors were assessed daily, with particular attention during the perioperative period after hard antler removal and antler tissue collection. Predefined humane endpoints included severe body-weight loss (>15–20% of initial body weight), marked reduction in food intake for more than 24–48 h, inability to stand or move normally, persistent bleeding, severe wound infection, dehydration, or severe or unrelieved pain/distress. Animals reaching these criteria would be examined by a veterinarian and removed from the experiment for treatment or humane euthanasia if necessary. No animals reached the predefined humane endpoints, no severe adverse events or procedure-related mortality occurred, and no animals were euthanized in this study. Hard antler removal and subsequent antler mesenchymal tissue collection were performed by experienced personnel under aseptic conditions. Before the procedure, anesthesia and perioperative analgesia were provided with xylazine hydrochloride (working concentration: 100 mg/mL; 1.0–1.5 mg/kg, intramuscular [IM]) followed by ketamine hydrochloride (working concentration: 50 mg/mL; 2–4 mg/kg, IM). After clipping and aseptic preparation of the antler base, a tourniquet was applied around the pedicle to minimize blood loss. The antler was transected just above the pedicle coronet (approximately 2 cm above the pedicle) using a sterile fine-toothed saw, taking care to avoid pedicle injury. Hemostasis was confirmed before gradual release of the tourniquet, and the stump was treated with topical antiseptic and protected according to animal-welfare guidelines. Antler mesenchymal tissue was dissected under sterile conditions; part of the tissue was fixed for immunofluorescence, and the remaining tissue was placed in PBS for RMC isolation. Following sample collection, atipamezole hydrochloride (working concentration: 5 mg/mL; 0.1–0.2 mg/kg, IM) was administered to reverse the effects of xylazine, and animals were monitored until full recovery.

2.2 RMCs Isolation and Culture

RMCs were isolated following an established protocol [20], and antler reserve mesenchymal layer (Fig. 1A) was minced and digested with 0.2% type II collagenase (093186, Gibco, Grand Island, NY, USA) at 37 °C for 2 h. After removing collagenase, digested complexes were cultured in growth medium consisting of Dulbecco's Modified Eagle Medium (DMEM, 6125246, Gibco, Grand Island, NY, USA) supplemented with 10% fetal bovine serum (FBS, F8318, Sigma-Aldrich, St. Louis, MO, USA) and 1% penicillin-streptomycin (15140-122, Gibco, Grand Island, NY, USA) at 37 °C in a humidified incubator with 5% CO_2. Cells from passages 3–5 were used for all experiments. The identity of the primary cells was validated by flow cytometric analysis of surface markers. Mycoplasma contamination was tested using the Myco-Lum™ Luminescent Mycoplasma Detection Kit for Low Sensitivity Instrument (Beyotime, C0297S). The B/A ratio was 0.76, which is below

the negative threshold of 0.9 according to the kit instructions; therefore, the cells were considered mycoplasma-negative.

2.3 Immunofluorescence

Antler tissue was fixed in 4% paraformaldehyde at 4 °C for 24 h, decalcified in decalcification solution at room temperature with solution changes every 3 days, then dehydrated through graded ethanol, cleared in xylene and embedded in paraffin. Sections (4 µm) were cut with a rotary microtome, mounted on poly-L-lysine–coated slides and dried. For immunofluorescence, sections were deparaffinized in xylene, rehydrated through descending ethanol to water, and subjected to antigen retrieval in 10 mM citrate buffer (pH 6.0) by microwave heating for about 10 min. After cooling, sections were washed with PBS, permeabilized with 0.3% Triton X-100 (P0096, Beyotime, Shanghai, China) and blocked with 10% normal goat serum for 30 min at room temperature. Slides were incubated with CD90 (27178-1-AP, dilution 1:500; Proteintech, Wuhan, China) and Ki67 (27309-1-AP, dilution 1:500; Proteintech, Wuhan, China) antibody at 4 °C overnight, washed, and then incubated with a fluorophore-conjugated secondary antibody (A0453, dilution 1:500; Beyotime, Shanghai, China) for 1 h in the dark. Nuclei were counterstained with DAPI (ZE0815, Vector Laboratories, Newark, CA, USA), and sections were mounted with anti-fade medium. Images were captured using a fluorescence microscope under identical settings, and fluorescence signals were analyzed with ImageJ software (Version 1.53t, National Institutes of Health, Bethesda, MD, USA). All animal samples were coded by a third party who was not involved in the histological quantification, and the histological quantification was performed in a blinded manner to avoid subjective bias.

RMCs were cultured in a 24-well cell culture dish for immunofluorescence. Cells were incubated with the indicated primary antibodies CD44 (5675-1-AP, dilution 1:500; Proteintech, Wuhan, China), CD105 (10862-1-AP, dilution 1:500; Proteintech, Wuhan, China) or β-catenin (P35222, dilution 1:1000; Cell Signaling Technology, Danvers, MA, USA) overnight at 4 °C. Samples were incubated with appropriate Alexa Fluor-conjugated secondary antibodies (A0453, dilution 1:500; Beyotime, Shanghai, China) and counterstained with DAPI. Images were captured using an inverted fluorescence microscope (Nikon, Tokyo, Japan). For quantification of β-catenin nuclear localization, 5 random fields of view were captured per group from three independent experiments. Nuclear β-catenin positive cells were defined as cells showing clear overlap between β-catenin fluorescence and the DAPI stained nucleus. The total number of cells and the number of nuclear β-catenin positive cells were counted in each field, and the percentage of nuclear β-catenin positive cells was calculated as nuclear positive cells divided by total cells multiplied by 100. Quantification was performed in a blinded manner using ImageJ software.

2.4 Characterization of RMCs

To examine the differentiation ability of RMCs, osteogenic and chondrogenic differentiation was induced *in vitro*. Briefly, cells were seeded at 5×10^5 cells per well in 6-well plates, and differentiation was started after they attained 80% confluence. For osteogenic differentiation, cells were cultured in osteogenic induction medium. The medium included DMEM, 10% FBS, 1% P/S, 100 nM dexamethasone, 10 mM β-glycerophosphate, 50 µM ascorbic acid. For chondrogenic differentiation, cells were cultured in chondrogenic differentiation medium supplemented with DMEM, 5% FBS, 1% P/S, 10 ng/mL transforming growth factor-beta 1 (TGF-β1, R&D Systems, Minneapolis, MN, USA), 50 µM ascorbic acid, 1% insulin-transferrin-selenium (ITS, OriCell, Guangzhou, China) for 1 week. For adipogenic differentiation, cells were cultured in adipogenic induction medium supplemented with DMEM, 10% FBS, 1% P/S, 1 µM dexamethasone (D4902, Sigma-Aldrich, St. Louis, MO, USA), 200 µM indomethacin (I7378, Sigma-Aldrich, St. Louis, MO, USA), 10 µg/mL insulin (I6634, Sigma-Aldrich, St. Louis, MO, USA), and 0.5 mM 3-Isobutyl-1-methylxanthine (IBMX, I5879, Sigma-Aldrich, St. Louis, MO, USA) for two days, followed by incubation in adipogenic maintenance medium (DMEM, 10% FBS, 1% P/S, 10 µg/mL insulin) for one day. This cycle was repeated 7–8 times. Subsequently, staining was performed using alizarin red (C0138, Beyotime, Shanghai, China), Alcian blue (ALCB-10001, Cyagen, Suzhou, Jiangsu, China) and Oil red O (C0158S, Beyotime, Shanghai, China) solutions, respectively. Images were captured using a fluorescence microscope (Nikon Corporation, Tokyo, Japan).

Flow cytometry was performed to assess the expression of CD44 and CD105 in isolated RMCs. Cells were harvested, washed with PBS, and incubated with the corresponding primary antibodies or isotype controls, followed by incubation with the appropriate fluorescent secondary antibody. After washing, the cells were analyzed using a flow cytometer (BD Biosciences, San Jose, CA, USA), and the data were processed with FlowJo software (Version 10.8, BD Biosciences, Ashland, OR, USA). Positive gates were set according to the isotype control.

2.5 Cell Proliferation Assays

To assess the effect of Arg on RMCs proliferation, cells were treated with various L-Arg concentrations in an L-Arg-deficient basal medium (MA0545, Meilunbio, Dalian, Liaoning, China). L-Arg (A8094, Sigma-Aldrich, St. Louis, MO, USA) was dissolved in PBS to prepare a stock solution and then diluted into the Arg-deficient basal medium to the indicated final concentrations (0, 200, 400,

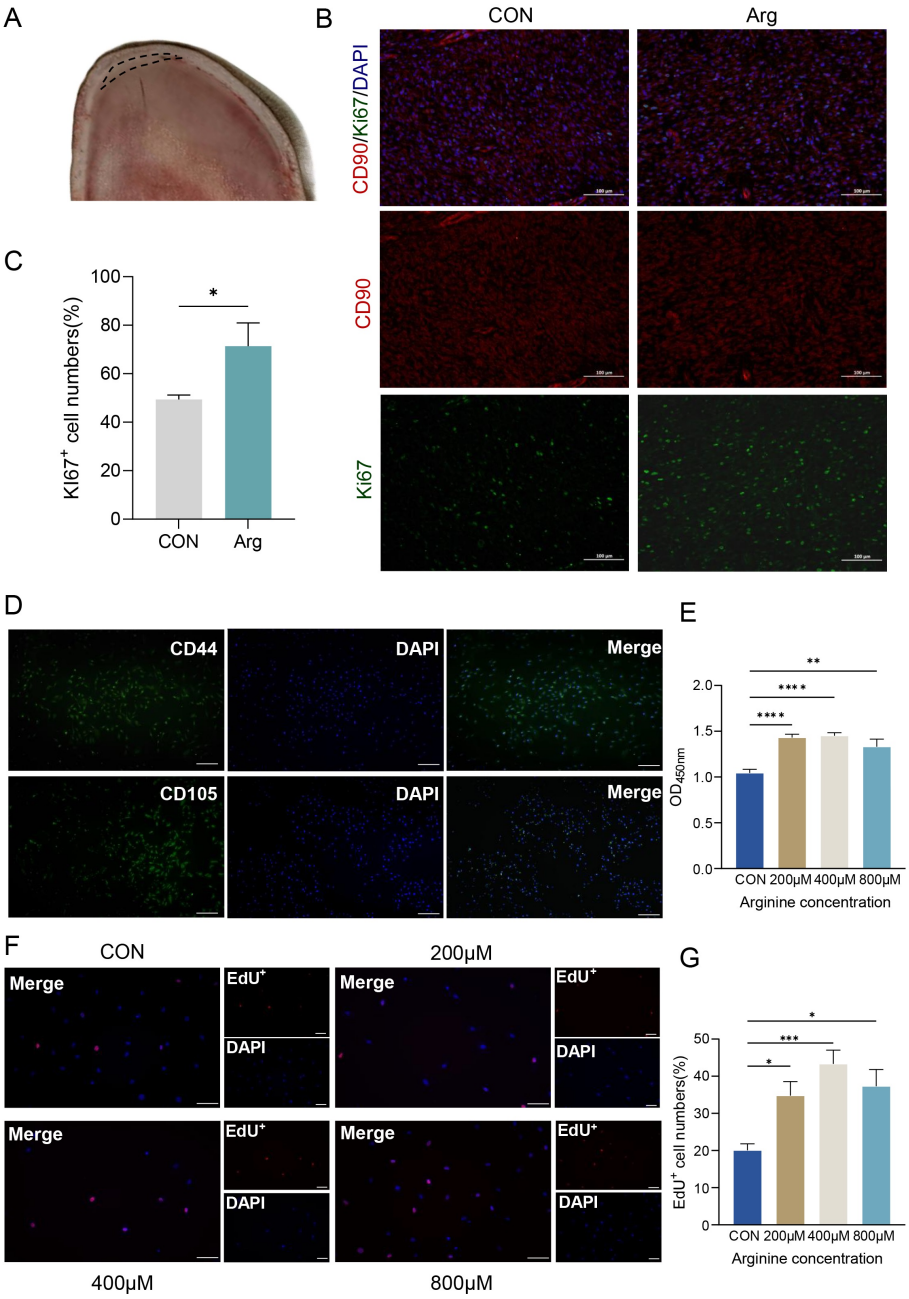

Fig. 1. Arginine promotes the proliferation of RMCs *in vivo* and *in vitro*. (A) Schematic diagram of the antler sampling site. (B) Sections were co-stained for the proliferation marker Ki67 (green) and the mesenchymal marker CD90 (red). Nuclei are counterstained with DAPI (blue). Scale bar, 100 μm. (C) Quantitative analysis of the percentage of Ki67-positive cells from images in (A,B). Data are presented as mean ± SEM (n = 3). *$p < 0.05$ vs. CON group (Student's *t*-test). (D) Immunofluorescence characterization of isolated and cultured RMCs, showing positive expression of mesenchymal stem cell surface markers CD44 and CD105. Nuclei are stained with DAPI (blue). Scale bar, 200 μm. (E) CCK-8 assay showing the viability of RMCs treated with 0 (CON), 200, 400, or 800 μM arginine for 48 h. **$p < 0.01$, ****$p < 0.0001$ compared to the CON group (one-way ANOVA with Tukey's post-hoc test). (F) Representative fluorescence images of EdU (red) incorporation in RMCs treated with 0 (CON), 200, 400, or 800 μM arginine for 48 h. Nuclei are stained with DAPI (blue). Scale bar, 100 μm. (G) Quantitative analysis of the percentage of EdU-positive cells from images in (F). Data are presented as mean ± SEM (n = 3). *$p < 0.05$, ***$p < 0.001$ compared to the CON group (one-way ANOVA with Tukey's post-hoc test). RMCs, reserve mesenchymal cells; DAPI, 4′,6-diamidino-2-phenylindole; SEM, Standard Error of the Mean; EdU, EdU (5-Ethynyl-2′-deoxyuridine) incorporation assay.

and 800 μM). Control cells received the same volume of vehicle. RMCs were seeded in 96-well plates at a density of 3×10^3 cells per well. Cell viability was evaluated at 48 h using the Cell Counting Kit-8 (CCK8, HY-K0301, MedChemExpress (MCE), Monmouth Junction, NJ, USA) according to the manufacturer's instructions. Absorbance was measured at 450 nm with a microplate reader. Proliferating cells were labeled with the BeyoClick™ 5-Ethynyl-2′-deoxyuridine (EdU) Cell Proliferation Kit with AF555 (C0076S, Beyotime, Shanghai, China). Briefly, RMCs treated with Arg for 48 h were incubated with 10 μM EdU for 2 h. After fixation and permeabilization, cells were stained with the Click iTRAQ reagent at room temperature in the dark for 30 min, then counterstained with Hoechst 33342 for nuclear staining. Images were acquired using a fluorescence microscope, and the percentage of EdU-positive cells was calculated from five randomly selected fields per well. EdU and CCK-8 assays were performed independently, using different batches of RMC cultures (3 independent batches), and each assay was repeated 3 times independently to ensure the reliability of the results. The cell seeding density and treatment conditions were consistent between the two assays.

2.6 RNA Sequencing and Bioinformatic Analysis

For RNA Sequencing (RNA-seq), cells cultured under proliferative conditions were treated with 400 μM Arg, which showed the strongest pro-proliferative effect. Total RNA was extracted from control and 400 μM Arg-treated RMCs (n = 3 biological replicates per group) using TRIzol reagent (RE34142520, Invitrogen, Carlsbad, California, USA). RNA integrity was confirmed with an Agilent 2100 Bioanalyzer (RIN >8.0). Library construction and 150-bp paired-end sequencing were performed on an Illumina HiSeq 4000 by Novogene Co., Ltd. Raw reads were processed with fastp for quality control. Clean reads were aligned to the Sika deer reference genome (*Cervus nippon*, PRJCA001220) using HISAT2 (Version 2.2.1, Daehwan Kim, University of Texas Southwestern Medical Center, Dallas, TX, USA) [21]. Gene expression levels were quantified from the alignment files and used for differential expression analysis. Differential expression analysis was performed using the DESeq2 package in R (Version 1.53.0, Michael Love, Simon Anders, Wolfgang Huber, Bioconductor, Boston, MA, USA) [22], with genes satisfying $|\log_2\text{FoldChange}| > 0.5$ and p-value < 0.05 considered significantly differentially expressed. Principal component analysis (PCA) was employed to assess the overall transcriptional variation between the Arg and Con groups. Kyoto Encyclopedia of Genes and Genomes (KEGG) pathway enrichment was performed using the clusterProfiler package (Version 4.21.0, Guangchuang Yu, Bioconductor, Boston, MA, USA) [23], applying an false discovery rate (FDR) threshold of <0.05 for significance.

2.7 Chondrogenic Differentiation

Micromass cultures were used to assess Arg's effect on RMCs chondrogenic differentiation [24]. Briefly, 1.5×10^5 cells in 10 μL medium were seeded as micromass droplets per well. After 1 h of adherence at 37 °C, 500 μL of chondrogenic differentiation medium containing L-Arg was added. The groups received L-Arg at final concentrations of 0, 200, 400, or 800 μM. After 4 d, samples were fixed for Alcian blue staining or collected for gene and protein analyses. Since 800 μM Arg showed the strongest promotive effect on chondrogenic differentiation, this concentration was used in the subsequent pathway perturbation experiments with rapamycin (RAPA) and a Wnt/β-catenin signaling pathway activator (CHIR99021).

2.8 Quantitative Real-Time PCR

Total RNA was reverse transcribed using the PrimeScript RT reagent Kit (RR037A, Takara, Kusatsu, Shiga, Japan). Quantitative Real-Time PCR (qRT-PCR) was performed on a CFX96 Touch system (CFX96 Touch System, Bio-Rad, Hercules, CA, USA) using TB Green Premix Ex Taq II (RR820A, Takara, Kusatsu, Shiga, Japan). Gene expression was normalized to glyceraldehyde-3-phosphate dehydrogenase (GAPDH) and quantified using the $2^{-\Delta\Delta Ct}$ method. The primer sequences are listed as follows: *SOX9* forward, 5′-CAAGAACAAGCCGCACGTCAAG-3′, and *SOX9* reverse, 5′-TCTCGCTCTCGTTCAGCAGTCT-3′; *COL2A1* forward, 5′-GTGGAGCAGCAAGAGCAAGGA-3′, and *COL2A1* reverse, 5′-AGCAGGCGGAGGAAGGTCAT-3′; *LEF1* forward, 5′-CGGGTGGTGTTGGACAGATTAC-3′, and *LEF1* reverse, 5′-GCGTTACGATGGCTGGATGAG-3′; *AXIN2* forward, 5′-GGCGATCAGGACGGTGCTTA-3′, and *AXIN2* reverse, 5′-GCTTGGAGACGATGCTGTTGTT-3′; *GAPDH* forward, 5′-AGATGGTGAAGGTCGGAGTG-3′, and *GAPDH* reverse, 5′-CCTTTCCATTGATGACGAGC-3′.

2.9 Western Blotting

Total protein was extracted using RIPA lysis buffer. Equal amounts of protein (20 μg) were separated by sodium dodecyl sulfate-polyacrylamide gel electrophoresis (SDS-PAGE), transferred to polyvinylidene difluoride (PVDF, IPVH00010, MilliporeSigma, Burlington, MA, USA) membranes, and blocked. Membranes were incubated overnight at 4 °C with primary antibodies. The following primary antibodies were used: rabbit COL2A1 (ab307674, dilution 1:1000; Abcam, UK), rabbit SOX9 (P48436, dilution 1:1000; Cell Signaling Technology, Danvers, MA, USA), rabbit mTOR (28273-1-AP, dilution 1:5000; Proteintech, Wu Han, China), rabbit p-mTOR (5536T, dilution 1:1000; Cell Signaling Technology, Danvers, MA, USA), rabbit p70 S6 Kinase (2708T, dilution 1:1000; Cell Signaling Technology, Danvers, MA, USA); rabbit p-p70 S6 Kinase (Thr389) (9234T, dilution 1:1000;

Cell Signaling Technology, Danvers, MA, USA), mouse β-catenin (8480T, dilution 1:1000; Cell Signaling Technology, Danvers, MA, USA), mouse GAPDH Antibody (MAB374, dilution 1:20,000; Sigma-Aldrich, St. Louis, MO, USA), followed by incubation with anti-rabbit IgG horseradish peroxidase (HRP, P0948; dilution 1:500; Beyotime, Shanghai, China) or anti-mouse IgG HRP (P0946, dilution 1:500; Beyotime, Shanghai, China). Finally, blot signals were detected using a chemiluminescence kit (26619, Thermo Fisher Scientific, Altrincham, Cheshire, UK) and imaged with a multifunctional imaging system (Tanon, Shanghai, China). Relative protein levels were normalized to the GAPDH level on the same blot. Proteins were analyzed in grayscale using ImageJ software to obtain quantitative data.

2.10 Statistical Analysis

All quantitative data are presented as mean $\pm$ standard error of the mean (SEM) from at least three independent experiments. Statistical comparisons among multiple groups were analyzed using one-way analysis of variance (ANOVA) followed by Tukey's post hoc test in GraphPad Prism (Version 9.0, GraphPad Software, San Diego, CA, USA). p-value < 0.05 was considered statistically significant.

3. Results

3.1 Arg Promotes the Proliferation of RMCs In Vitro and In Vivo

The antler reserve mesenchymal layer in the antler growth center was selected for analysis (Fig. 1A). CD90 and Ki67 double immunofluorescence staining were performed in this region (Fig. 1B). CD90 (red) labels the mesenchymal stem cells, Ki67 (green) labels proliferating cells, and DAPI (blue) stains the nuclei. Compared with the control group, the Arg group showed a marked increase in the proportion of Ki67-positive cells among CD90-positive cells, with stronger green fluorescence signals overall. Quantitative analysis (Fig. 1C) revealed that Arg treatment significantly increased the proportion of $Ki67^+$ cells ($p < 0.05$). These results indicate that dietary Arg supplementation markedly enhances cell proliferation in the antler mesenchymal cell region.

The primary cultured cells displayed a typical spindle-shaped morphology (**Supplementary Fig. 1A**). Immunofluorescence (Fig. 1D) and flow cytometric analysis (**Supplementary Fig. 1B**) showed high expression of CD44 and CD105, and multilineage differentiation assays confirmed their osteogenic (**Supplementary Fig. 1C**), and chondrogenic (**Supplementary Fig. 1D**) and adipogenic (**Supplementary Fig. 1E**) differentiation potential. Together, these findings indicate that the isolated cells possess mesenchymal stem cell characteristics. The CCK-8 assay demonstrated that Arg treatment increased cell viability compared with the control group, with the 400 µM group exhibiting the strongest effect (Fig. 1E, $p < 0.05$). EdU staining further showed that the percentage of EdU-positive cells was significantly higher in the Arg-treated groups than in the CON group, indicating that Arg promotes DNA synthesis in RMCs (Fig. 1F,G, $p < 0.05$). Overall, these results suggest that Arg enhances the proliferation of RMCs.

3.2 Transcriptomic Profiling Identifies Arg-Responsive Genes and Pathways Associated With Proliferation and Chondrogenic Programs

To identify the molecular pathways by which Arg promotes RMCs proliferation, we performed RNA-seq analysis on cells from both the control group and the 400 µM Arg-treated group. PCA revealed a clear separation between the two groups, indicating distinct global transcriptional profiles, with PC1 and PC2 together accounting for 67.78% of the total variance (Fig. 2A). Differential expression analysis using $|\log_2 FC| > 0.5$ and $p < 0.05$ identified 2907 differentially expressed genes (DEGs) after Arg treatment, including 1388 upregulated genes and 1519 downregulated genes. Among the upregulated DEGs, *SST*, *UBE2C*, *PLK1*, *PCLAF*, and *FAM83D* were markedly increased, while *DES*, *TGFB1*, *CSPG4*, and *KIFC1* showed notable decreases among the downregulated DEGs (Fig. 2B). KEGG pathway enrichment analysis revealed the upregulated DEGs were significantly enriched in multiple canonical signaling pathways, including ECM-receptor interactions, focal adhesion, axon guidance, Hippo signaling pathways, mTOR signaling pathways, osteoclast differentiation, PI3K-Akt signaling pathways, and Wnt signaling pathways (Fig. 2C). Downregulated DEGs were mainly enriched for pathways related to DNA replication, cellular senescence, nucleocytoplasmic transport, the proteasome, oxidative phosphorylation, p53 signaling pathways, nucleotide metabolism, and the cell cycle (Fig. 2C). Next, to intuitively illustrate how DEGs are distributed across pathways and to explore potential inter-pathway connections, we built a gene-pathway conceptual network. Using pathways significantly enriched by upregulated genes and those already linked to antler growth and chondrogenesis, we visualized DEGs mapped to ECM–receptor interaction, focal adhesion, Wnt signaling, mTOR signaling, and osteoclast differentiation (Fig. 2D). The network topology showed that ECM–receptor interaction and focal adhesion occupied central hubs, connecting many DEGs and forming a closely linked cluster with Wnt signaling, mTOR signaling, and osteoclast differentiation, highlighting extracellular matrix-adhesion signaling as a core part of the Arg-induced transcriptional response. Within this cluster, numerous ECM/adhesion-related components (e.g., *FN1*, *LAMA1*/*LAMA3*, *COL1A2*/*COL4A3*/*COL6A1*, and various integrins *ITGA*/*ITGB*) were densely represented, supporting extensive remodeling of cell-matrix interactions following Arg treatment. Additionally, key Wnt receptors and ligands, like *FZD1*, *FZD2*, *WNT5A*, *WNT10B*, and

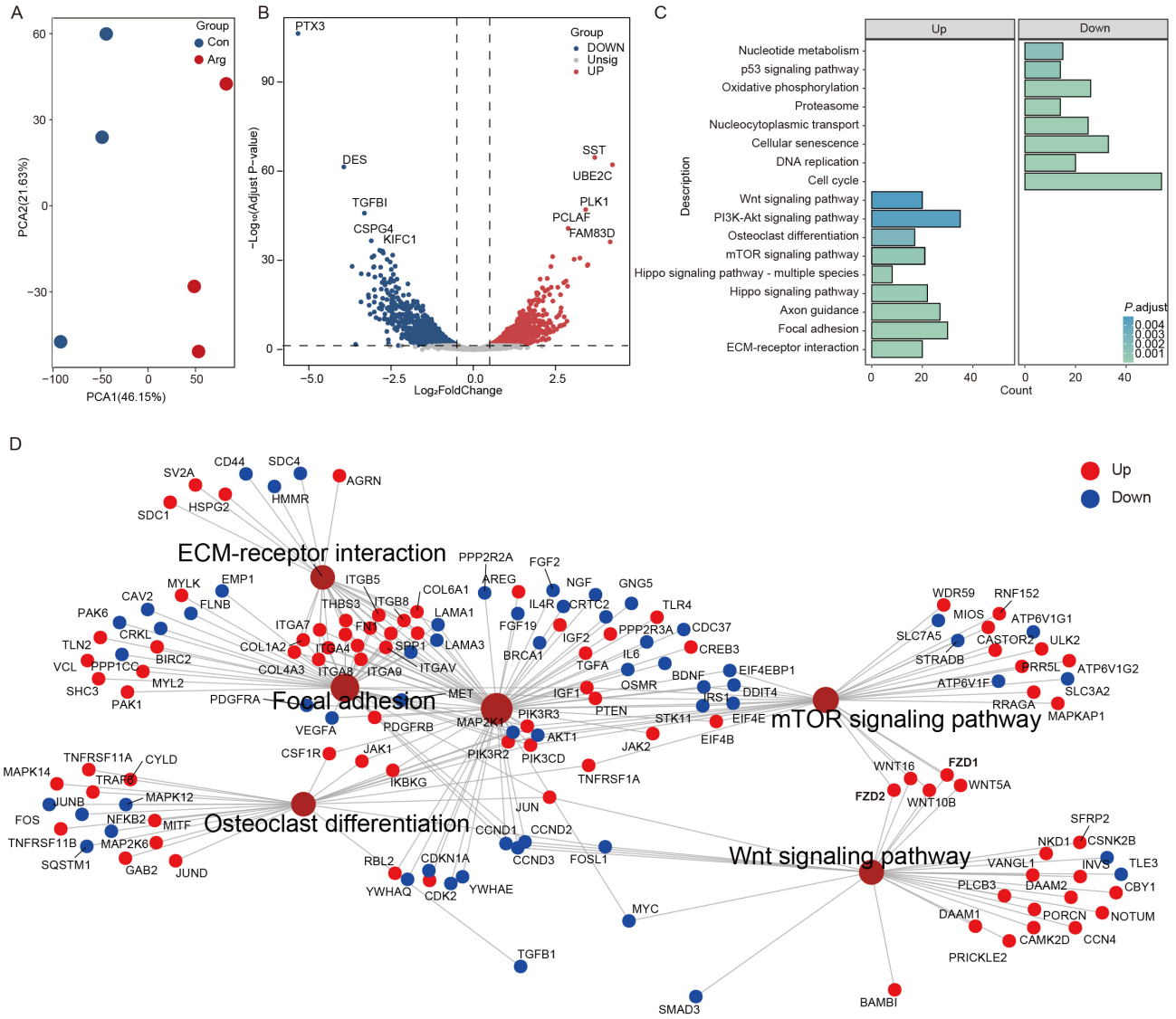

Fig. 2. Transcriptomic profiling of RMCs in response to arginine treatment. (A) PCA plot showing distinct transcriptional profiles between the CON and Arg groups. (B) Volcano plot of differentially expressed genes (DEGs). Significantly upregulated (red) and downregulated (blue) genes are highlighted. (C) KEGG pathway enrichment analysis of upregulated and downregulated DEGs (based on $|\log_2 FC| > 0.5$ and $p < 0.05$). (D) Gene-pathway interaction network. Nodes represent DEGs, colored by their expression change (red: up, blue: down), and are mapped to their significantly enriched KEGG pathways (grey circles). PCA, Principal component analysis; KEGG, Kyoto Encyclopedia of Genes and Genomes.

WNT16, showed overall upregulation, indicating activation of Wnt signaling. In addition, several nutrient-sensing and translation-related nodes associated with mTOR signaling (e.g., *CASTOR2*, *RRAGA*, *EIF4E*, *EIF4EBP1*, *EIF4B*, *SLC7A5*/*SLC3A2*) displayed significant differential expression, pointing to mTOR-regulated processes involved in the Arg response. Overall, the gene-pathway network analysis indicates that Arg-driven transcriptional changes are organized around an ECM-adhesion hub and are linked with Wnt/mTOR growth-regulating pathways, providing systems-level support for Arg's pro-proliferative effects in RMCs (Fig. 2D). Overall, the results suggest that Arg treatment significantly remodels the RMCs transcriptome. These changes are linked to the coordinated modulation of ECM/adhesion-related signaling and key growth-regulatory pathways, which may play a role in Arg-driven RMC proliferation and chondrogenic biological processes.

3.3 Effects of Arg on Chondrogenic Differentiation of RMCs

To validate the role of Arg in promoting commitment of RMCs to the chondrogenic lineage, an *in vitro* chondrogenic induction system was supplemented with different concentrations of Arg and cell differentiation was subsequently induced for 4 d. Alcian blue staining revealed that cells treated with 200 μM, 400 μM, or 800 μM Arg showed

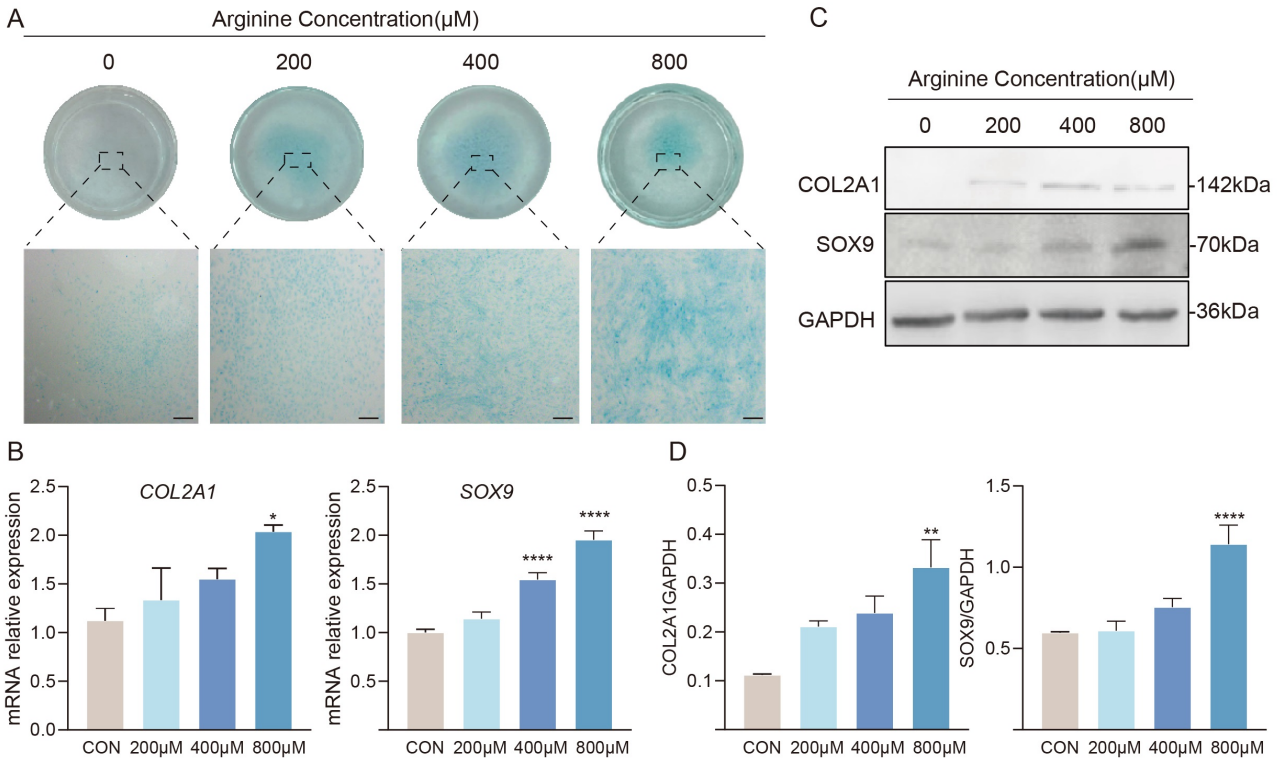

Fig. 3. Arginine enhances chondrogenic differentiation of RMCs. (A) Alcian Blue staining of micromass cultures after 4 d chondrogenic induction with the indicated concentrations of arginine, showing increased proteoglycan deposition (n = 3). Scale bar, 800 µm. (B) Relative mRNA expression levels of chondrogenic marker genes COL2A1 and SOX9 as determined by qRT-PCR. Data are presented as mean ± SEM (n = 3). *$p < 0.05$; ****$p < 0.0001$ compared to CON group (one-way ANOVA with Tukey's test). (C,D) Western blot analysis of COL2A1 and SOX9 protein expression after arginine treatment (n = 3). **$p < 0.01$; ****$p < 0.0001$ compared to CON group (one-way ANOVA with Tukey's test). GAPDH served as the loading control. qRT-PCR, Quantitative Real-Time PCR; COL2A1, Collagen type II alpha 1 chain; SOX9, SRY-box transcription factor 9; GAPDH, Glyceraldehyde-3-phosphate dehydrogenase.

a significantly larger staining area compared to the CON group, indicating increased cartilage matrix deposition and a higher level of chondrogenic differentiation (Fig. 3A). Similarly, qPCR (Fig. 3B) and Western blot (Fig. 3C,D) analyses confirmed that Arg treatment markedly increased both the mRNA and protein levels of the key chondrogenic markers SOX9 and COL2A1. Overall, these findings demonstrate that Arg boosts the chondrogenic differentiation potential of RMCs.

3.4 Arg Activates mTOR Signaling During Chondrogenic Differentiation of RMCs

To determine whether mTOR signaling contributes to Arg-induced chondrogenesis, we performed pharmacological perturbation experiments during chondrogenic induction. The phosphorylation levels of mTOR and its downstream target S6K were analyzed after Arg treatment. Western blot analysis showed that Arg increased the p-mTOR/mTOR and p-S6K/S6K ratios during chondrogenic differentiation, indicating enhanced mTOR signaling under Arg treatment (Fig. 4A,B).

To further assess the role of mTOR activity, RAPA (an inhibitor of mTOR signaling) was applied during chondrogenic induction. Alcian blue staining revealed that Arg promoted the deposition of cartilage matrix, whereas this effect was attenuated by RAPA (Fig. 4C). Consistent with this observation, the mRNA expression levels of SOX9 and COL2A1 were increased in the Arg group, but reduced in the Arg+RAPA group (Fig. 4D). Western blot analysis further showed that RAPA decreased the p-S6K/S6K ratio and attenuated Arg-induced upregulation of SOX9 and COL2A1 (Fig. 4E,F). Together, these results suggest that mTOR activity is involved in the Arg-enhanced chondrogenic differentiation of RMCs.

3.5 Activation of Canonical Wnt/β-catenin Signaling Attenuates Arg-Enhanced Chondrogenic Differentiation of RMCs

To examine Wnt/β-catenin signaling during chondrogenic differentiation, β-catenin immunofluorescence and gene expression analyses were performed after Arg treatment. Immunofluorescence staining showed that nuclear β-catenin fluorescence was reduced after Arg treatment and was lowest at a concentration of 800 µM (Fig. 5A and

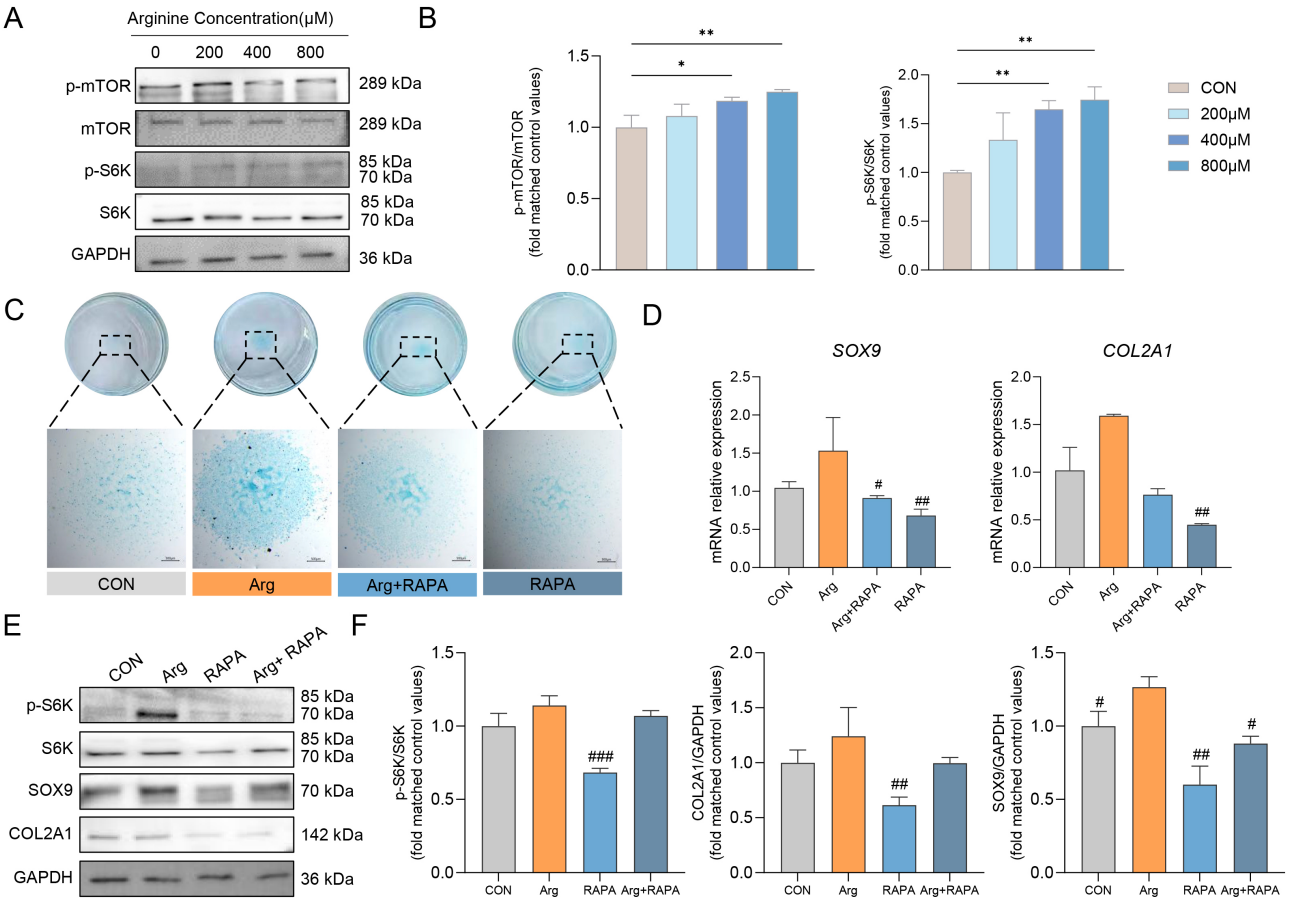

Fig. 4. Arg activates mTOR signaling during chondrogenic differentiation of RMCs. (A) Western blot analysis of p-mTOR, mTOR, p-S6K, and S6K in RMCs treated with different concentrations of Arg. (B) Quantification of the p-mTOR/mTOR and p-S6K/S6K ratios (n = 3). (C) Alcian blue staining of chondrogenic differentiation in the CON, Arg, Arg+RAPA, and RAPA groups (n = 3). Scale bar, 500 μm. (D) Relative mRNA expression of SOX9 and COL2A1 in the CON, Arg, Arg+RAPA, and RAPA groups (n = 3). Western blot analysis (E) and quantification (F) of p-S6K/S6K, SOX9, and COL2A1 protein expression in the CON, Arg, Arg+RAPA, and RAPA groups (n = 3). Data are presented as mean ± SEM. For panel (B), statistical significance was determined relative to the control group. For panels (D,F), $^{\#}$ indicates comparison with the Arg group. $^{*}p < 0.05$, $^{**}p < 0.01$; $^{\#}p < 0.05$, $^{\#\#}p < 0.01$, $^{\#\#\#}p < 0.001$.

Supplementary Fig. 2A). Western blot analysis revealed the effect of Arg on total β-catenin expression was non-monotonic, with increased β-catenin expression at 200 and 400 μM, but decreased expression at 800 μM (Fig. 5B,C). In addition, the canonical Wnt target genes *Axin2* and *LEF1* were modulated by Arg treatment and showed lower expression at 800 μM (Fig. 5D). Together, these results suggest that canonical Wnt/β-catenin signaling was attenuated by 800 μM Arg during chondrogenic differentiation.

To further investigate the role of Wnt/β-catenin signaling in Arg-mediated chondrogenic differentiation, CHIR99021 (CHIR, a Wnt/β-catenin signaling pathway activator) was applied during chondrogenic induction. Alcian blue staining showed that 800 μM Arg promoted cartilage matrix deposition, with the effect attenuated by CHIR (Fig. 5E). Consistent with this finding, the mRNA expression levels of SOX9 and COL2A1 were increased in the Arg group but reduced in the Arg+CHIR group (Fig. 5F). Moreover, CHIR increased the expression levels of *LEF1* and *Axin2* (Fig. 5G), which showed a similar trend to nuclear β-catenin accumulation (Fig. 5H and **Supplementary Fig. 2B**). Western blot analysis further showed that CHIR increased β-catenin protein expression and reduced the Arg-induced upregulation of SOX9 and COL2A1 (Fig. 5I,J). Together, these results suggest that activation of Wnt/β-catenin signaling attenuates the promotive effect of Arg on the chondrogenic differentiation of RMCs.

4. Discussion

Deer antlers represent a unique mammalian model of rapid organ regeneration. They are characterized by rapid cartilage formation that originates from the growth center reserve mesenchyme, where mesenchymal progenitors undergo substantial expansion and chondrogenic commitment to support antler growth [1]. Arg is a conditionally essential amino acid with established roles in nu-

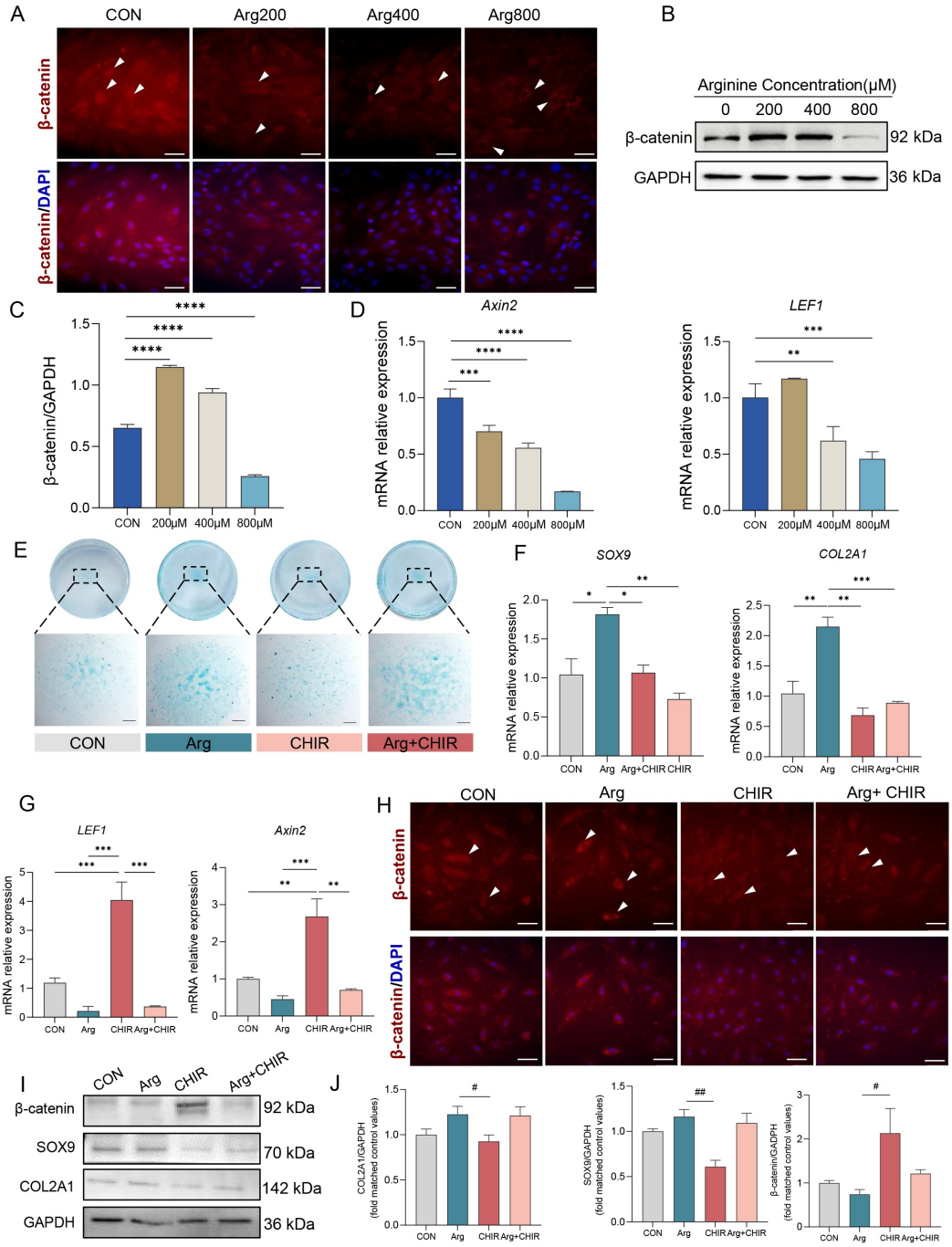

Fig. 5. Effects of Arg and CHIR on the Wnt/β-catenin signaling during chondrogenic differentiation of RMCs. (A) Immunofluorescence staining of nuclear β-catenin in RMCs treated with different concentrations of Arg (n = 3). Scale bar, 50 μm. (B) Western blot analysis and quantification (C) of total β-catenin protein expression after Arg treatment (n = 3). (D) Relative mRNA expression of Axin2 and LEF1 in RMCs treated with different concentrations of Arg (n =3). (E) Alcian blue staining of chondrogenic differentiation in the CON, Arg, CHIR, and Arg+CHIR groups (n = 3). Scale bar, 500 μm. (F) Relative mRNA expression of SOX9 and COL2A1 in the CON, Arg, CHIR, and Arg+CHIR groups (n = 3). (G) Relative mRNA expression of Axin2 and LEF1 in the CON, Arg, CHIR, and Arg+CHIR groups (n = 3). (H) Immunofluorescence staining and quantification of nuclear β-catenin in the CON, Arg, CHIR, and Arg+CHIR groups (n = 3). Scale bar, 50 μm. Western blot analysis (I) and quantification (J) of β-catenin, SOX9, and COL2A1 protein expression in the CON, Arg, CHIR, and Arg+CHIR groups (n = 3). Data are presented as mean ± SEM. The white arrows in panels A and H indicate representative RMCs showing different levels of nuclear β-catenin staining. For panels (C,D), $^{**}p < 0.01$, $^{***}p < 0.001$, $^{****}p < 0.0001$ indicates comparison with the CON group. For panels (F–J), $^{*}p < 0.05$, $^{**}p < 0.01$, $^{***}p < 0.001$ indicates comparison with the CON group. $^{\#}p < 0.05$, $^{\#\#}p < 0.01$ vs. the Arg group.

trient sensing and stem/progenitor cell function. In the present study, we showed that Arg significantly enhances the *in vitro* proliferation of RMCs, as evidenced by increased cell viability and DNA synthesis [15,25]. Transcriptomic profiling further revealed that Arg induces coordinated remodeling of ECM adhesion programs and multiple growth- and differentiation-related signaling networks, in line with the central role of cell-ECM interactions in regulating chondrocyte lineage behaviors [26]. Functionally, Arg also potentiates chondrogenic differentiation, as evidenced by enhanced cartilage-like matrix deposition and increased SOX9/COL2A1 expression. Additional activity-related and pharmacological analyses also suggest that Arg modulates Wnt/β-catenin signaling and activates mTOR signaling during chondrogenic differentiation.

The pro-proliferative effect of Arg observed by CCK-8 and EdU assays aligns with the broader idea that amino acid availability can promote stem/progenitor cell expansion by linking metabolic supply to growth-control signaling, primarily through nutrient-sensitive pathways such as mTORC1 [27]. Additionally, several upregulated DEGs in Arg-treated RMCs (including *UBE2C*, *PLK1*, *PCLAF*, and *FAM83D*) are well-known cell-cycle regulators involved in DNA synthesis and mitotic progression, thus providing a transcriptional basis for the increased DNA synthesis observed with EdU staining. *UBE2C* promotes correct cell-cycle progression [28,29]; *PLK1* is crucial for multiple mitotic steps [30]; *PCLAF* regulates DNA synthesis via *PCNA* interaction [31]; and *FAM83D* is involved in spindle organization and efficient cell-cycle progression [32]. At the pathway level, enrichment of PI3K-Akt, Hippo, and mTOR signaling among the upregulated gene sets indicates that Arg may activate multiple interconnected growth-control pathways that coordinate nutrient status, biosynthesis needs, and cell-cycle progression [27,33]. KEGG enrichment analysis revealed that the downregulated DEGs were mainly associated with pathways related to DNA replication, cell cycle, cellular senescence, and p53 signaling. However, the enrichment of downregulated genes in these categories should be interpreted with caution, since these pathways include not only proliferation-associated genes but also checkpoint- and growth-restraining regulators such as *CDKN1A*, *CDKN2B*, *CDKN2C*, *CDKN2D*, *GADD45A*, and *TGFB1*. Therefore, the proliferative effect of Arg was interpreted primarily on the basis of phenotypic assays, including Ki67 staining, CCK-8, and EdU incorporation. Notably, the enrichment of osteoclast differentiation-related terms might reflect shared remodeling-related transcriptional programs rather than direct osteoclast formation in RMCs. However, this aligns with the broader regenerative process of antler growth, where rapid endochondral ossification and coordinated tissue remodeling are essential, and osteoclast-related activities are closely linked to regeneration and bone turnover [34,35].

A key feature of the transcriptomic response is an ECM-adhesion hub, with ECM-receptor interactions and focal adhesion at its core, thus connecting many DEGs. This indicates that Arg-induced transcriptional changes are partly centered on cell-ECM interactions [36]. Mechanistically, ECM components (e.g., collagens, laminins, fibronectin) and their receptors (integrins) regulate adhesion and migration and transmit extracellular mechanical cues into intracellular signaling through integrin adhesion complexes and focal adhesions, thereby driving mechanotransduction and shaping downstream gene expression programs [37]. Matrix stiffness, adhesion-site availability, and integrin-mediated cytoskeletal tension are well known to influence proliferation-differentiation decisions in mesenchymal stem cells. Chondrogenic commitment is particularly sensitive to mechanical and adhesive microenvironmental cues [38]. Importantly, ECM-adhesion signaling intersects with PI3K-Akt, Hippo (YAP/TAZ), and mTOR networks, providing a plausible systems-level bridge linking ECM cues with growth and nutrient-sensing regulation, consistent with the coordinated pathway enrichment observed in our dataset [33,39,40]. In the physiological context of antler development, rapid tissue reconstruction requires sustained cell expansion, migration, and massive matrix deposition, making ECM remodeling and adhesion dynamics biologically essential. Therefore, the ECM-adhesion hub identified here provides a coherent link between Arg-responsive transcriptional programs and key processes underlying the rapid development of antler cartilage [41].

At the functional level, Arg significantly enhanced the chondrogenic differentiation of RMCs. The increased Alcian blue–positive area indicates greater accumulation of sulfated glycosaminoglycans/proteoglycans, providing direct evidence of cartilage-like matrix formation [42]. This phenotypic change was supported by molecular assays showing increased mRNA and protein levels of SOX9 and COL2A1. SOX9 is a master transcription factor for chondrogenesis and drives the expression of significant cartilage matrix genes, including COL2A1 [43]. Therefore, concurrent upregulation of the SOX9-COL2A1 axis is a hallmark of activated chondrogenic programming [6]. Notably, these differentiation outcomes align with the transcriptomic enrichment of ECM/adhesion modules. During chondrogenesis, ECM remodeling and cell–matrix interactions not only shape the microenvironment required for condensation and tissue assembly, but also influence the efficiency of matrix synthesis and deposition [44]. Accordingly, Arg-induced upregulation of ECM and adhesion-related components may provide a favorable structural and signaling context that supports enhanced cartilage matrix accumulation.

With respect to the pathway signals suggested by transcriptomics, it is important to interpret the Wnt/mTOR findings conservatively. RNA-seq enrichment indicates that Wnt- and mTOR-related gene sets are transcriptionally responsive to Arg treatment, but enrichment alone does not

establish pathway activation [27,45]. An important point requiring careful interpretation is that the effect of Arg on β-catenin was not concentration-dependent across all tested doses. While mTOR signaling increased progressively with increasing Arg concentration, β-catenin showed a non-monotonic pattern, increasing at 200 and 400 µM, but decreasing at 800 µM. Therefore, our data do not support a uniform, concentration-dependent suppression of canonical Wnt/β-catenin signaling. Instead, the decrease in β-catenin was observed specifically under the condition of 800 µM Arg, which was also accompanied by enhanced chondrogenic differentiation. These results indicate a possible association between reduced β-catenin expression and the pro-chondrogenic effect of Arg at this concentration. At the protein level, Arg modulated β-catenin expression and increased the phosphorylation of mTOR and S6K, suggesting that Arg-induced chondrogenic differentiation is accompanied by the suppression of Wnt/β-catenin signaling and enhancement of mTOR-associated anabolic regulation [27]. These observations are biologically plausible, given the stage-dependent roles of Wnt/β-catenin signaling in mesenchymal stem cell chondrogenesis, where reduced β-catenin activity often stabilizes chondrogenic phenotypes and matrix production [46]. This interpretation is further supported by well-established antagonistic interactions between SOX9 and β-catenin/Wnt signaling during chondrogenesis [47]. Moreover, mTOR functions as a central nutrient-sensing hub that coordinates protein synthesis and cell growth, consistent with the observed increases in chondrogenic markers and matrix deposition [27]. Notably, mTORC1 has been reported to regulate chondrogenic progression via preferential translational control of SOX9 [48]. Taken together, our results indicate that Arg may coordinate nutrient-sensitive anabolic regulation (mTOR-associated) with lineage-associated signaling changes (reduced canonical Wnt/β-catenin), thereby biasing RMCs toward a cellular state that is favorable for chondrogenesis.

Although we incorporated pharmacological perturbation experiments and additional activity-related readouts, including the p-S6K1/S6K1 ratio, nuclear localization of β-catenin, and LEF1/AXIN2 expression, more direct genetic approaches would further strengthen the mechanistic interpretation. Moreover, although our *in vitro* model demonstrates the intrinsic responsiveness of RMCs to Arg, it does not fully recapitulate the complex antler growth microenvironment, which includes dynamic mechanical cues, ECM remodeling, and multicellular interactions. Validation in more physiologically relevant systems, such as 3D cultures, co-culture systems, or tissue-level models, is needed to further assess the role of Arg in cartilage formation and antler regeneration.

5. Conclusions

In summary, this study found that Arg promotes the proliferation of deer RMCs both *in vivo* and *in vitro*, and enhances their chondrogenic differentiation potential. During chondrogenic induction, 800 µM Arg was associated with attenuation of canonical Wnt/β-catenin signaling and activation of mTOR signaling, accompanied by increased SOX9 and COL2A1 expression and enhanced cartilage matrix formation. These findings suggest that Arg acts as an important nutritional regulator of antler growth, likely by coordinating RMC proliferation and chondrogenic differentiation in association with changes in Wnt/β-catenin and mTOR signaling. Our results provide a basis for further investigation of Arg supplementation in deer production.

Availability of Data and Materials

The datasets used and analyzed during the current study are available from the corresponding author on reasonable request.

Author Contributions

This study involved the following contributions: Investigation: RD, HLL, YZ, and XD; Validation: WN, RD, XD, and HHL; Formal analysis: HHL and YZ; Writing—original draft preparation: RD, HLL, and WN; Writing—review and editing, Visualization, and Funding acquisition: HS. All authors contributed to editorial changes in the manuscript. All authors read and approved the final manuscript. All authors have participated sufficiently in the work and agreed to be accountable for all aspects of the work.

Ethics Approval and Consent to Participate

The experimental protocol was approved by the Animal Ethics Committee of Jilin Agricultural University (Approval ID: 20220614005). Animal testing follows the 3R (Replacement, Reduction, Refinement) principle and the ARRIVE guidelines, the Regulations for the Administration of Affairs Concerning Experimental Animals of China, the national standard Laboratory Animal—Environment and Housing Facilities (GB 14925-2010), and the Guidelines for Ethical Review of Laboratory Animal Welfare (GB/T 35892-2018).

Acknowledgment

Not applicable.

Funding

This work was funded by the National Key Research and Development Program of China (2023YFD1302000), the Science and Technology Development Program from Jilin Province (20230101271JC), the Jilin Agricultural Research System (JLARS-2025-080205), and the Science and Technology Research Project of the Jilin Provincial Department of Education (JJKH20261452KJ).

Conflicts of Interest

The authors declare no conflicts of interest.

Supplementary Material

Supplementary material associated with this article can be found, in the online version, at https://doi.org/10.31083/FBL50041.

References

[1] Qin T, Zhang G, Zheng Y, Li S, Yuan Y, Li Q, *et al*. A population of stem cells with strong regenerative potential discovered in deer antlers. Science (New York, N.Y.). 2023; 379: 840–847. https://doi.org/10.1126/science.add0488.

[2] Ba H, Wang D, Yau TO, Shang Y, Li C. Transcriptomic analysis of different tissue layers in antler growth Center in Sika Deer (Cervus nippon). BMC Genomics. 2019; 20: 173. https://doi.org/10.1186/s12864-019-5560-1.

[3] Wang YS, Chu WH, Zhai JJ, Wang WY, He ZM, Zhao QM, *et al*. High quality repair of osteochondral defects in rats using the extracellular matrix of antler stem cells. World Journal of Stem Cells. 2024; 16: 176–190. https://doi.org/10.4252/wjsc.v16.i2.176.

[4] Li C, Clark DE, Lord EA, Stanton JAL, Suttie JM. Sampling technique to discriminate the different tissue layers of growing antler tips for gene discovery. The Anatomical Record. 2002; 268: 125–130. https://doi.org/10.1002/ar.10120.

[5] Upadhyay U, Kolla S, Chelluri LK. Extracellular matrix composition analysis of human articular cartilage for the development of organ-on-a-chip. Biochemical and Biophysical Research Communications. 2023; 667: 81–88. https://doi.org/10.1016/j.bbrc.2023.04.117.

[6] Song H, Park KH. Regulation and function of SOX9 during cartilage development and regeneration. Seminars in Cancer Biology. 2020; 67: 12–23. https://doi.org/10.1016/j.semcancer.2020.04.008.

[7] Bell DM, Leung KK, Wheatley SC, Ng LJ, Zhou S, Ling KW, *et al*. SOX9 directly regulates the type-II collagen gene. Nature Genetics. 1997; 16: 174–178. https://doi.org/10.1038/ng0697-174.

[8] Szuwart T, Kierdorf H, Kierdorf U, Clemen G. Ultrastructural aspects of cartilage formation, mineralization, and degeneration during primary antler growth in fallow deer (Dama dama). Annals of Anatomy = Anatomischer Anzeiger: Official Organ of the Anatomische Gesellschaft. 1998; 180: 501–510. https://doi.org/10.1016/S0940-9602(98)80055-1.

[9] Sun Z, Guo SS, Fässler R. Integrin-mediated mechanotransduction. The Journal of Cell Biology. 2016; 215: 445–456. https://doi.org/10.1083/jcb.201609037.

[10] Dupont S. Role of YAP/TAZ in cell-matrix adhesion-mediated signalling and mechanotransduction. Experimental Cell Research. 2016; 343: 42–53. https://doi.org/10.1016/j.yexcr.2015.10.034.

[11] Wang N, Lu Y, Rothrauff BB, Zheng A, Lamb A, Yan Y, *et al*. Mechanotransduction pathways in articular chondrocytes and the emerging role of estrogen receptor-α. Bone Research. 2023; 11: 13. https://doi.org/10.1038/s41413-023-00248-x.

[12] Cynober L, Boucher JL, Vasson MP. Arginine metabolism in mammals. Journal of Nutritional Biochemistry. 1995; 6: 402–413. https://doi.org/10.1016/0955-2863(95)00066-9.

[13] Agostinelli E. Polyamines and transglutaminases: biological, clinical, and biotechnological perspectives. Amino Acids. 2014; 46: 475–485. https://doi.org/10.1007/s00726-014-1688-0.

[14] Bahadoran Z, Mirmiran P, Kashfi K, Ghasemi A. Endogenous flux of nitric oxide: Citrulline is preferred to Arginine. Acta Physiologica (Oxford, England). 2021; 231: e13572. https://doi.org/10.1111/apha.13572.

[15] Hou Q, Dong Y, Huang J, Liao C, Lei J, Wang Y, *et al*. Exogenous L-arginine increases intestinal stem cell function through CD90+ stromal cells producing mTORC1-induced Wnt2b. Communications Biology. 2020; 3: 611. https://doi.org/10.1038/s42003-020-01347-9.

[16] Witte MB, Barbul A. Arginine physiology and its implication for wound healing. Wound Repair and Regeneration: Official Publication of the Wound Healing Society [and] the European Tissue Repair Society. 2003; 11: 419–423. https://doi.org/10.1046/j.1524-475x.2003.11605.x.

[17] Gonzalez-Menendez P, Phadke I, Olive ME, Joly A, Papoin J, Yan H, *et al*. Arginine metabolism regulates human erythroid differentiation through hypusination of eIF5A. Blood. 2023; 141: 2520–2536. https://doi.org/10.1182/blood.2022017584.

[18] Si H, Liu H, Nan W, Li G, Li Z, Lou Y. Effects of Arginine Supplementation on Serum Metabolites and the Rumen Bacterial Community of Sika Deer (*Cervus nippon*). Frontiers in Veterinary Science. 2021; 8: 630686. https://doi.org/10.3389/fvets.2021.630686.

[19] Fennessy PF. Deer Antlers: Regeneration, function and evolution . Journal of the Royal Society of New Zealand, 1984; 14: 290–291. https://doi.org/10.1080/03036758.1984.10426948.

[20] Wang D, Berg D, Ba H, Sun H, Wang Z, Li C. Deer antler stem cells are a novel type of cells that sustain full regeneration of a mammalian organ-deer antler. Cell Death & Disease. 2019; 10: 443. https://doi.org/10.1038/s41419-019-1686-y.

[21] Pertea M, Kim D, Pertea GM, Leek JT, Salzberg SL. Transcript-level expression analysis of RNA-seq experiments with HISAT, StringTie and Ballgown. Nature Protocols. 2016; 11: 1650–1667. https://doi.org/10.1038/nprot.2016.095.

[22] Love MI, Huber W, Anders S. Moderated estimation of fold change and dispersion for RNA-seq data with DESeq2. Genome Biology. 2014; 15: 550. https://doi.org/10.1186/s13059-014-0550-8.

[23] Yu G, Wang LG, Han Y, He QY. clusterProfiler: an R package for comparing biological themes among gene clusters. Omics: a Journal of Integrative Biology. 2012; 16: 284–287. https://doi.org/10.1089/omi.2011.0118.

[24] Stegen S, Rinaldi G, Loopmans S, Stockmans I, Moermans K, Thienpont B, *et al*. Glutamine Metabolism Controls Chondrocyte Identity and Function. Developmental Cell. 2020; 53: 530–544.e8. https://doi.org/10.1016/j.devcel.2020.05.001.

[25] Du T, Han J. Arginine Metabolism and Its Potential in Treatment of Colorectal Cancer. Frontiers in Cell and Developmental Biology. 2021; 9: 658861. https://doi.org/10.3389/fcell.2021.658861.

[26] Gao Y, Liu S, Huang J, Guo W, Chen J, Zhang L, *et al*. The ECM-cell interaction of cartilage extracellular matrix on chondrocytes. BioMed Research International. 2014; 2014: 648459. https://doi.org/10.1155/2014/648459.

[27] Meng D, Frank AR, Jewell JL. mTOR signaling in stem and progenitor cells. Development (Cambridge, England). 2018; 145: dev152595. https://doi.org/10.1242/dev.152595.

[28] Yamanaka A, Hatakeyama S, Kominami K, Kitagawa M, Matsumoto M, Nakayama K. Cell cycle-dependent expression of mammalian E2-C regulated by the anaphase-promoting complex/cyclosome. Molecular Biology of the Cell. 2000; 11: 2821–2831. https://doi.org/10.1091/mbc.11.8.2821.

[29] Nicolau-Neto P, Palumbo A, De Martino M, Esposito F, De Almeida Simão T, Fusco A, *et al*. UBE2C Is a Transcriptional Target of the Cell Cycle Regulator FOXM1. Genes (Basel). 2018; 9: 188. https://doi.org/10.3390/genes9040188.

[30] Iliaki S, Beyaert R, Afonina IS. Polo-like kinase 1 (PLK1) signaling in cancer and beyond. Biochemical Pharmacology. 2021; 193: 114747. https://doi.org/10.1016/j.bcp.2021.114747.

[31] Tantiwetrueangdet A, Panvichian R, Sornmayura P, Leelaudomlipi S, Macoska JA. PCNA-associated factor (KIAA0101/PCLAF) overexpression and gene copy number alterations in hepatocellular carcinoma tissues. BMC Cancer. 2021; 21: 295. https://doi.org/10.1186/s12885-021-07994-3.

[32] Fulcher LJ, He Z, Mei L, Macartney TJ, Wood NT, Prescott AR, *et al*. FAM83D directs protein kinase CK1α to the mitotic spindle for proper spindle positioning. The EMBO Reports. 2019; 20: e47495. https://doi.org/10.15252/embr.201847495.

[33] Borreguero-Muñoz N, Fletcher GC, Aguilar-Aragon M, Elbediwy A, Vincent-Mistiaen ZI, Thompson BJ. The Hippo pathway integrates PI3K-Akt signals with mechanical and polarity cues to control tissue growth. PLoS Biology. 2019; 17: e3000509. https://doi.org/10.1371/journal.pbio.3000509.

[34] Price JS, Allen S, Faucheux C, Althnaian T, Mount JG. Deer antlers: a zoological curiosity or the key to understanding organ regeneration in mammals? Journal of Anatomy. 2005; 207: 603–618. https://doi.org/10.1111/j.1469-7580.2005.00478.x.

[35] Feleke M, Bennett S, Chen J, Hu X, Williams D, Xu J. New physiological insights into the phenomena of deer antler: A unique model for skeletal tissue regeneration. Journal of Orthopaedic Translation. 2020; 27: 57–66. https://doi.org/10.1016/j.jot.2020.10.012.

[36] Han R, Han L, Wang S, Li H. Whole Transcriptome Analysis of Mesenchyme Tissue in Sika Deer Antler Revealed the CeRNAs Regulatory Network Associated With Antler Development. Frontiers in Genetics. 2020; 10: 1403. https://doi.org/10.3389/fgene.2019.01403.

[37] Chastney MR, Conway JRW, Ivaska J. Integrin adhesion complexes. Current Biology: CB. 2021; 31: R536–R542. https://doi.org/10.1016/j.cub.2021.01.038.

[38] Lv H, Li L, Sun M, Zhang Y, Chen L, Rong Y, *et al*. Mechanism of regulation of stem cell differentiation by matrix stiffness. Stem Cell Research & Therapy. 2015; 6: 103. https://doi.org/10.1186/s13287-015-0083-4.

[39] Su H, Tang X, Zhang X, Liu L, Jing L, Pan D, *et al*. Comparative proteomics analysis reveals the difference during antler regeneration stage between red deer and sika deer. PeerJ. 2019; 7: e7299. https://doi.org/10.7717/peerj.7299.

[40] Katoh K. Integrin and Its Associated Proteins as a Mediator for Mechano-Signal Transduction. Biomolecules. 2025; 15: 166. https://doi.org/10.3390/biom15020166.

[41] Liu R, Zhang P, Bai J, Zhong Z, Shan Y, Cheng Z, *et al*. Integrated Transcriptomic and Proteomic Analyses of Antler Growth and Ossification Mechanisms. International Journal of Molecular Sciences. 2024; 25: 13215. https://doi.org/10.3390/ijms252313215.

[42] Kipnes J, Carlberg AL, Loredo GA, Lawler J, Tuan RS, Hall DJ. Effect of cartilage oligomeric matrix protein on mesenchymal chondrogenesis in vitro. Osteoarthritis and Cartilage. 2003; 11: 442–454. https://doi.org/10.1016/s1063-4584(03)00055-4.

[43] Barbieri O, Astigiano S, Morini M, Tavella S, Schito A, Corsi A, *et al*. Depletion of cartilage collagen fibrils in mice carrying a dominant negative Col2a1 transgene affects chondrocyte differentiation. American Journal of Physiology. Cell Physiology. 2003; 285: C1504–C1512. https://doi.org/10.1152/ajpcell.00579.2002.

[44] Strecanska M, Danisovic L, Ziaran S, Cehakova M. The Role of Extracellular Matrix and Hydrogels in Mesenchymal Stem Cell Chondrogenesis and Cartilage Regeneration. Life (Basel). 2022; 12: 2066. https://doi.org/10.3390/life12122066.

[45] Wang X, Guan Y, Xiang S, Clark KL, Alexander PG, Simonian LE, *et al*. Role of Canonical Wnt/β-Catenin Pathway in Regulating Chondrocytic Hypertrophy in Mesenchymal Stem Cell-Based Cartilage Tissue Engineering. Frontiers in Cell and Developmental Biology. 2022; 10: 812081. https://doi.org/10.3389/fcell.2022.812081.

[46] Yang K, Wang X, Zhang H, Wang Z, Nan G, Li Y, *et al*. The evolving roles of canonical WNT signaling in stem cells and tumorigenesis: implications in targeted cancer therapies. Laboratory Investigation; a Journal of Technical Methods and Pathology. 2016; 96: 116–136. https://doi.org/10.1038/labinvest.2015.144.

[47] Topol L, Chen W, Song H, Day TF, Yang Y. Sox9 inhibits Wnt signaling by promoting beta-catenin phosphorylation in the nucleus. The Journal of Biological Chemistry. 2009; 284: 3323–3333. https://doi.org/10.1074/jbc.M808048200.

[48] Iezaki T, Horie T, Fukasawa K, Kitabatake M, Nakamura Y, Park G, *et al*. Translational Control of Sox9 RNA by mTORC1 Contributes to Skeletogenesis. Stem Cell Reports. 2018; 11: 228–241. https://doi.org/10.1016/j.stemcr.2018.05.020.